cated by excess sodium generally correspond with periods of high storm activity as determined from NOAA meteorological records (*17*). Apparently, storm activity creates enough tropospheric turbulence to transport marine aerosols to the midtroposphere. Periods of high sea sodium preceded occurrences of the dust in 1980 and 1981; however, the sea sodium peaks are lower in 1982. This suggest that fewer strong storms occurred throughout the Pacific basin and Asia, resulting in less dust being transported to Hawaii in 1982. Also, changes in air mass trajectories may be responsible for the decrease in 1982.

Asian dust appears to come in waves and the concentration peaks are fairly symmetrical, probably because of meteorological conditions where the dust originated. Such processes would tend to transport dust in waves, which could have a duration of several days as observed in other, shorter term studies at MLO (*5, 7*). The actual peak concentrations of dust could thus be much higher than the weekly average concentrations of this study which appear in Fig. 1.

Upslope samples collected during 1979 and 1980 support the downslope filter results (*14*). During cleaner months, crustal concentrations in these samples are about three times higher than in downslope samples (*14*) and to some extent appear to represent local basaltic particles, as noted above. Yet when the dust occurs crustal material is often found in higher concentrations in downslope samples. This suggests that the Asian dust is in higher concentration above the altitude of MLO, which supports Shaw's observation (*5*) that the dust occurred in a layer above the altitude of MLO; thus, downslope wind would bring dust from closer to the center of this dust layer to MLO than would upslope winds. Prospero *et al.* (*1*) found similar results in that Saharan dust became well mixed throughout the troposphere above the marine boundary layer, with some more stratified layers in existence after transport over several thousand kilometers. A similar situation may occur in this case.

In conclusion, the Asian dust events in the Pacific occur consistently in the spring, generally peaking in late April and early May. These events account for most of the crustal material, which amounts to about five times more yearly crustal mass then would be present if the events did not occur. This large influx may be a significant contribution to sedimentation rates in the Pacific, as suggested by others (*4, 18*).

The dust events observed in this study are consistent with results of other studies at MLO and in the Pacific. Bodhaine *et al.* (*3*) observed maxima in b_{sp} during the spring of each year from 1974 to 1980. The 1979 and 1980 b_{sp} data contain increases that correspond to peaks in Fig. 1 and are obviously due to Asian dust. Part of the Sea-Air Exchange (SEAREX) program involves study of Asian dust events in the Pacific (*18*); results of 1981 sampling on Oahu show six peaks that are very similar in concentration and time of occurrence to our results.

JOSEF R. PARRINGTON
WILLIAM H. ZOLLER
NAMIK K. ARAS
Department of Chemistry, University of Maryland, College Park 20742

References and Notes

1. J. M. Prospero, R. A. Glaccum, R. T. Nees, *Nature (London)* **289**, 570 (1981).
2. L. Schutz, *Ann. N.Y. Acad. Sci.* **338**, 515 (1980).
3. B. A. Bodhaine, B. G. Mendonca, J. M. Harris, J. M. Miller, *J. Geophys. Res.* **86**, 7395 (1981).
4. R. A. Duce, C. K. Unni, B. J. Ray, J. M. Prospero, J. T. Merrill, *Science* **209**, 1522 (1980).
5. G. E. Shaw, *J. Appl. Meteorol.* **19**, 1254 (1980).
6. K. A. Rahn, R. D. Borys, G. E. Shaw, *Nature (London)* **268**, 713 (1977).
7. M. Darzi and J. W. Winchester, *J. Geophys. Res.* **87**, 1251 (1982).
8. W. C. Cunningham and W. H. Zoller, *J. Aerosol. Sci.* **12**, 367 (1981).
9. B. G. Mendonca and W. T. Iwaoka, *J. Appl. Meteorol.* **8**, 213 (1969).
10. B. A. Bodhaine and R. F. Pueschel, *J. Geophys. Res.* **77**, 5106 (1972).
11. H. J. Simpson, *ibid.*, p. 5266.
12. B. G. Mendonca, *J. Appl. Meteorol.* **8**, 533 (1969).
13. M. S. Germani *et al.*, *Anal. Chem.* **52**, 240 (1980).
14. J. R. Parrington and W. H. Zoller, in preparation.
15. K. Govindaraju, *Geostandards Newslett.* **5**, 31 (1981).
16. S. R. Taylor, *Geochim. Cosmochim. Acta* **28**, 1273 (1964).
17. Meteorological data supplied by B. A. Bodhaine, National Oceanic and Atmospheric Administration.
18. M. Uematsu, R. A. Duce, R. McDonald, J. Williams, *SEAREX Newslett.* **4** (September 1981).
19. Supported by NOAA grant NA79RAC00050. We thank the staff at the National Bureau of Standards (NBS) instrumentation division, headed by J. K. Whittaker, for their help in equipment design, and the staff at the NBS reactor for providing space and use of the facilities in analyses. We also thank K. Coulson and the staff at Mauna Loa Observatory for their help in maintaining equipment and changing samples. Results presented here are from a dissertation to be submitted to the graduate school, University of Maryland, by J.R.P. in partial fulfillment of the requirements for the Ph.D. degree in chemistry.

18 August 1982; revised 19 January 1983

Argonne Intense Pulsed Neutron Source Used to Solve the Molecular Structure of a Novel Organometallic Complex

Abstract. *The single-crystal structure of* $Mn(CO)_3(C_7H_{11})$ *is the first to be solved by direct methods based on time-of-flight neutron diffraction data obtained at the Argonne Intense Pulsed Neutron Source. The molecule contains an unusual three-center, two-electron manganese-hydrogen-carbon interaction.*

The application of single-crystal neutron diffraction techniques to chemical problems that have a bearing on C–H bond activation is a relatively new and potentially fruitful area of research. Although the pioneering structural work (*1*) was done by x-ray diffraction because of the small size of the crystals, neutron diffraction is preferable since it provides accurate hydrogen atom positional and thermal parameters without the systematic C–H bond shortening obtained with x-ray diffraction. Using neutron diffraction, we have characterized a number of molecules with elongated C–H bonds due to "activation" of the bond by a nearby metal (*2, 3*). These studies provide bonding models that can improve our understanding of chemical reactivity and catalytic processes (*4*). We now report the neutron diffraction structure of methylcyclohexenylmanganese tricarbonyl, $Mn(CO)_3(C_7H_{11})$; the key feature of this structure is the intramolecular interaction of the manganese atom with an aliphatic C–H bond.

To our knowledge, this is the first single-crystal structure to be independently solved on the basis of time-of-flight (TOF) neutron data from a pulsed neutron source. The data were obtained at the Argonne Intense Pulsed Neutron Source (IPNS) (*5*) with a new single-crystal instrument based on the TOF Laue technique (*6*). We believe these results represent a seminal achievement in the advancement of an important new structure determination method.

The ability to obtain neutron diffraction data is often limited by the low flux available from neutron sources. Furthermore, with conventional instruments only a small percentage of the available neutrons are selected with a monochromator, and the remainder are wasted. Neutrons are produced at IPNS by a spallation process in which high-energy (500-MeV) protons are accelerated into a uranium target in small bursts at 30 times per second to generate very high peak neutron fluxes (*5*). Because of the pulsed nature of the source, nearly the entire spectrum of moderated neutrons is used by application of TOF techniques to determine the de Broglie wavelength $\lambda = (h/m\ell)t$, where h is Planck's constant, m is the neutron mass, ℓ is the source-to-detector path length, and t is the time of flight.

The single-crystal instrument at IPNS consists of a conventional crystal orienter with low-temperature (15 to 300 K) capabilities. The major component is a unique two-dimensional (30 by 30 cm active area), position-sensitive ^{6}Li-glass scintillation neutron detector (*7*), which has a spatial (x,y) resolution of 3.5 mm and is placed 25 to 35 cm from the sample. Data are initially stored in the 2.5-megabyte memory of a microcomputer as a three-dimensional (x,y,t) histogram containing possibly hundreds of Bragg reflections. Several (15 to 30) such histograms are needed to collect a complete data set. The user has the option of displaying the data as shown in Fig. 1, where the x-y grid of intensity data for a selected wavelength range is shown.

A crystal of $Mn(CO)_3(C_7H_{11})$ (*8, 9*), with dimensions of 4.0 by 1.5 by 1.0 mm^3, was used to collect 25 x,y,t histograms at 25 K, each of which contains ~ 100 Bragg reflections for a total of 2642 peaks. A least-squares fit of the positions of 595 peaks gave unit cell parameters at 25 K of a = 6.431(5) Å, b = 9.720(2) Å, c = 16.890(9) Å, and β (crystallographic angle between a and c) = 111.21(5)° (the number in parentheses is the standard deviation of the least significant figure). The systematic absences are unique for the monoclinic space group $P2_1/c$. The observed structure factor amplitudes, $F_0{}^2$, were derived from integrated counts by application of corrections for the λ dependencies of the incident neutron flux, the detector efficiency, absorption, and a $\lambda^4/\sin^2\theta$ factor, where θ is the Bragg angle. Many such factors are constant with monochromatic incident radiation, but with multiwavelength data they must be calculated or empirically measured as a function of λ.

After an initial failure to phase the data with the previously determined room-temperature x-ray structure (*9*) because of an unpropitious choice of unit cell (*10*), the low-temperature structure was solved independently on the basis of the TOF data with the direct methods program MULTAN (*11*). In spite of the large proportion of negative scattering amplitudes b ($b_{Mn} = 0.39 \times 10^{-12}$ cm; $b_H = -0.374 \times 10^{-12}$ cm; $\Sigma b^2_{Mn,H}/\Sigma b^2_{all} = 0.24$) and the prediction that this might prevent a solution by direct methods (*12*), the structure solution proceeded smoothly in support of our earlier observations (*13*). At the present stage of refinement, with isotropic thermal parameters and a secondary extinction parameter, the discrepancy index $R(F_o)$ is 0.12. The good agreement between the positional parameters for nonhydrogen atoms derived from the x-ray and neutron data is convincing evidence of the reliability of the TOF technique. The atomic thermal parameters have refined to very small or negative values, in part because of the low sample temperature but also because one or more of the λ-dependent factors is probably not being evaluated accurately (*14*).

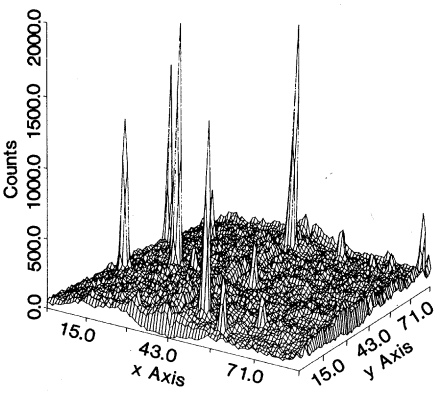

Fig. 1. A portion of a time-of-flight neutron Laue histogram from a crystal of $Mn(CO)_3(C_7H_{11})$. The units for the x and y axes are channel numbers corresponding to horizontal and vertical positions on the detector (30 by 30 cm area). The neutron counts for each x,y channel have been summed over ten time channels corresponding to a wavelength range of 1.94 to 2.18 Å.

The most important feature of the structure is the Mn–C(1)–H(1A) interaction characterized by a very long C(1)–H(1A) distance of 1.19(1) Å, with Mn–H(1A) = 1.84(1) Å and Mn–C(1) = 2.34(1) Å (Fig. 2). The average value for the other C–H distances is, as expected, 1.09(1) Å. The H(1A) is located almost exactly in an octahedral site about the manganese atom, with H(1A)–Mn–C(8) = 87.4(3)°, H(1A)–Mn–C(9) = 87.7(4)°, and H(1A)–Mn–C(10) = 174.0(2)° (see Fig. 2). If this interaction is ignored, the molecule formally contains 16 valence electrons. An 18-electron configuration is achieved only by delocalization of the two electrons in the C(1)–H(1A) bond to form a three-center, two-electron C(1)–H(1A)–Mn bond. This same type of interaction was structurally characterized in the iron-cyclooctenyl complex $\{Fe[P(OCH_3)_3]_3(\mu^3\text{-}C_8H_{13})\}(BF_4)$, with C–H = 1.164(3) Å and Fe–H = 1.874(3) Å (*2*). The remainder of the interatomic distances in $Mn(CO)_3(C_7H_{11})$ are quite normal [average values: Mn–CO, 1.809(7) Å, C–O, 1.154(9) Å; Mn–C, 2.12(6) Å; C–C(sp^2), 1.41(1) Å; and C–C(sp^3), 1.534(3) Å].

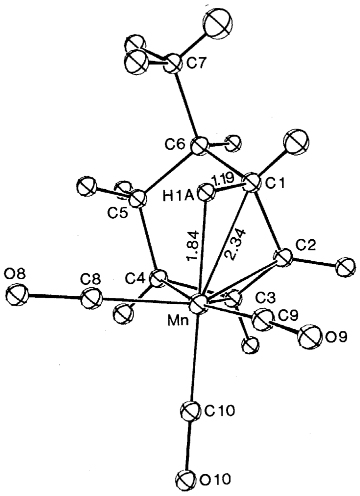

Fig. 2. The molecular structure of $Mn(CO)_3(C_7H_{11})$ obtained with neutron time-of-flight diffraction data at 25 K. The dimensions of the ellipsoids were chosen for reasons of clarity.

The structure represents the intermediate (**b**) in the interconversion between a metal-allyl complex (**a**) and a metal-dienehydride complex (**c**):

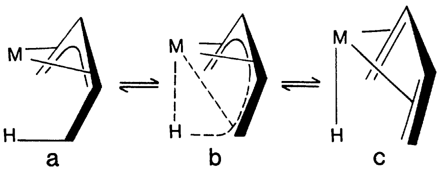

Additional evidence in support of structure **b** is derived from the short C(1)–C(2) distance of 1.507(4) Å relative to C(4)–C(5) = 1.535(5) Å, which indicates the partial multiple-bond character of the former.

The elucidation of this mode of C–H bond activation lends insight into mechanisms for catalytic activation and functionalization of saturated hydrocarbons and has been used for stoichiometric electrophilic substitution reactions at the bridged carbon (*8, 9*). The reverse reaction, C–H bond formation, is equally important. We believe that structural information of the sort presented here will lead to useful models for the mode of transfer of hydrogen from metal to ligands, an important process in the metal-catalyzed reduction of CO.

ARTHUR J. SCHULTZ
RAYMOND G. TELLER
MARK A. BENO
JACK M. WILLIAMS

Chemistry Division,
Argonne National Laboratory,
Argonne, Illinois 60439

M. BROOKHART
W. LAMANNA
M. BETH HUMPHREY

Department of Chemistry,
University of North Carolina,
Chapel Hill 27514

References and Notes

1. F. A. Cotton, T. LaCour, A. G. Stanislowski, *J. Am. Chem. Soc.* **96**, 754 (1974); F. A. Cotton and V. W. Day, *Chem. Commun.* **1974**, 415 (1974).
2. R. K. Brown, J. M. Williams, A. J. Schultz, G. D. Stucky, S. D. Ittel, R. L. Harlow, *J. Am. Chem. Soc.* **102**, 981 (1980).
3. A. J. Schultz, R. K. Brown, J. M. Williams, R. R. Schrock, *ibid.* **103**, 169 (1981); M. A. Beno, J. M. Williams, M. Tachikawa, E. L. Muetterties, *ibid.*, p. 1485.
4. R. Ugo, *Catal. Rev.-Sci. Eng.* **11**, 225 (1975).
5. J. M. Carpenter, *Nucl. Instrum. Methods* **145**, 91 (1977); ______, D. L. Price, N. J. Swanson, "IPNS—a national facility for condensed matter research" (Report ANL-78-88, Argonne National Laboratory, Argonne, Ill., 1978).
6. S. W. Peterson, A. H. Reis, Jr., A. J. Schultz, P. Day, *Solid State Chemistry: A Contemporary Overview*, S. L. Holt, J. B. Milstein, M. Robbins, Eds. (Advances in Chemistry Series 186, American Chemical Society, Washington, D.C., 1980), pp. 75–91; A. J. Schultz, R. G. Teller, S. W. Peterson, J. M. Williams, in *Neutron Scattering—1981*, J. Faber, Ed. (AIP Conference Proceedings Number 89, American Institute of Physics, New York, 1982), pp. 35–41.
7. M. G. Strauss, R. Brenner, F. J. Lynch, C. B. Morgan, *IEEE Trans. Nucl. Sci.* **NS-28**, 800 (1981).
8. W. Lamanna and M. Brookhart, *J. Am. Chem. Soc.* **103**, 989 (1981).
9. M. Brookhart, W. Lamanna, M. B. Humphrey, *ibid.* **104**, 2117 (1982).
10. After solving the low-temperature neutron structure, we derived the transformations $\mathbf{a}_n = -\mathbf{a}_x$, $\mathbf{b}_n = -\mathbf{b}_x$, and $\mathbf{c}_n = 2\mathbf{a}_x + \mathbf{c}_x$, where the subscripts refer to the original neutron and x-ray unit-cell vectors. Because of the fortuitous near-equivalencies of the magnitudes of $c_n = 17.132$ Å and $\beta_n = 113.21°$ with $c_x = 17.250$ Å and $\beta_x = 112.00°$, we initially thought the unit cells were equivalent and attempted to use the x-ray atomic coordinates to phase the neutron data. At the time, not understanding the lack of success, we proceeded to solve the neutron structure independent of the x-ray data.
11. J. P. Declercq, G. Germain, P. Main, M. M. Woolfson, *Acta Crystallogr. Sect. A* **29**, 231 (1973).
12. S. K. Sikka, *ibid.* **25**, 539 (1969).
13. R. W. Broach, A. J. Schultz, J. M. Williams, G. M. Brown, J. M. Manriquez, P. J. Fagan, T. J. Marks, *Science* **203**, 172 (1979).
14. An improved method for determining these factors is under study.
15. The work at Argonne National Laboratory was performed under the auspices of the Office of Basic Energy Science, Division of Materials Sciences, Department of Energy, under contract W-31-109-Eng-38. The work at the University of North Carolina was supported by NIH grant 5 R01 GM28938-02.

19 August 1982; revised 27 October 1982

Carbon Dioxide Exchange Between Air and Seawater: No Evidence for Rate Catalysis

Abstract. *It has been suggested that enzymatic catalysis plays a major role in regulating the mass transport of carbon dioxide from the atmosphere into the oceans. Evidence for this mechanism was not found in a series of gas exchange experiments in which the gas transfer rate coefficients for samples obtained from various natural seawaters, with and without the addition of carbonic anhydrase, were compared with those from artificial seawater. Wind-induced turbulence appears to be the major factor controlling the ocean's response to anthropogenic increases in atmospheric carbon dioxide.*

It is well recognized that uptake and regeneration of CO_2 in the oceans provide a major control on the chemistry of seawater, and the ultimate fate of excess atmospheric CO_2 lies largely in the oceans (*1*). Fickian transport of CO_2 across the air-sea interface can be accelerated by chemical reaction of aqueous CO_2 with components of the bicarbonate alkalinity system (*2*). At $p\mathrm{H} \leq 8$ the reaction $CO_2 + H_2O \rightarrow H_2CO_3 \rightarrow HCO_3^- + H^+$ (reaction 1) is important, whereas when the pH rises above 8 the reaction $CO_2 + OH^- \rightarrow HCO_3^-$ (reaction 2) increasingly contributes to the removal of CO_2 from solution until it dominates reaction 1 at $p\mathrm{H} > 10$ (*3*). Because a rise in pH leads to both a decrease in the partial pressure of aqueous CO_2 and the direct conversion of CO_2 to HCO_3^- by way of reaction 2, any possible chemical enhancement of CO_2 transport into seawater is strongly dependent on pH. In addition, the relative importance of chemical enhancement of CO_2 transport processes has been shown repeatedly to be an inverse function of wind-induced turbulence across the liquid surface (*4*). At the pH of seawater, which typically is about 8.0 to 8.2, and with the turbulence usually present at the ocean surface, CO_2 chemical reactivity is believed to play a minor role in the exchange of CO_2 between the atmosphere and the oceans (*5*). However, because reaction 1 is relatively slow (*3*), chemical enhancement could be important even at the pH of seawater, were catalysis of this reaction possible (*6*).

Berger and Libby (*7*), on the basis of experiments performed over a decade ago with samples from southern California coastal waters, concluded that carbonic anhydrase (CA), which is produced and excreted by numerous marine vertebrates and invertebrates, might be present in some oceanic areas in sufficient quantities to play an important role in regulating the exchange of atmospheric CO_2 with the oceans. We reexamined this hypothesis in a series of gas transfer experiments under rigid laboratory conditions. To determine whether CO_2 exchange with natural seawater was enhanced enzymatically, we compared, under a fixed mixing regime and in the presence or absence of commercially prepared bovine CA or ethoxyzolamide (an inhibitor of carbonic anhydrase activity), the pH-dependent gas transfer coefficients for various marine waters with those for an artificial seawater that was known not to have any catalytic properties (*8*).

Our gas-liquid exchange system consisted of (i) a circulating, closed-loop gas environment coupled through a nondispersing infrared spectrophotometer for continuous CO_2 analysis and (ii) an aqueous phase which was both temperature-controlled and mixed with a magnetic stirring bar to provide moderate turbulent diffusion. Once a steady-state atmospheric CO_2 concentration was established (*9*), the gas phase was opened to the aqueous phase and the rate of CO_2 transport between the two phases was measured over a period of 30 to 45 minutes to calculate a gas transfer rate coefficient (*10*). The starting atmospheric CO_2 concentration in all experiments was held at 1800 ppm to ensure that absorption of CO_2 into the liquid phase occurred under all our experimental conditions (*11*) and that the reservoir of CO_2 in the gas phase remained relatively unchanged during an experiment.

We first established the optimum liquid mixing regime in our gas exchange system to ensure that if catalysis of CO_2 transport took place, it could readily be observed. The gas transfer rate coefficient K (min^{-1}) at pH 8.10 was hardly affected by mixing speeds up to 500 rev/min, but then increased dramatically with further increases in mixing up to 700 rev/min, the maximum speed possible before the magnetic bar became unstable (Fig. 1). Addition of 0.5 to 20 mg of bovine CA per liter had no effect on K at either end of this range of mixing speeds, but at 500 rev/min we found a 60 percent increase in K with addition of CA at 0.5 mg/liter and a twofold increase with addition of the enzyme at ≥ 2 mg/liter. Hence, all subsequent experiments were performed with a constant mixing speed of 500 rev/min.

These results confirm the general conclusion that chemical reactivity between CO_2 and HCO_3^- has no impact on the overall mass transfer of CO_2 into solution when turbulence is high (*5*). Clearly, at 700 rev/min the surface film through which diffusion of CO_2 occurred was so thin, about 100 μm (*12*), that physical diffusion rather than chemical enhancement was the rate-limiting step, whereas at 500 rev/min the surface film thickness had increased to about 450 μm and chemical enhancement became important in the overall transport process.